Interfacial Metal Flux in Ligand Mixtures. 1. The Revisited Reaction Layer Approximation: Theory and Examples of Applications

Zeshi Zhang[§] and Jacques Buffle*

Analytical and Biophysical Environmental Chemistry (CABE), University of Geneva, Sciences II, 30 quai E. Ansermet, 1211 Geneva 4, Switzerland

Received: December 26, 2008; Revised Manuscript Received: February 26, 2009

Understanding the physical chemical behaviors of each metal species in a solution containing a mixture of ligands is a prerequisite, e.g., for studying metal bioavailability or making predictions on dynamic risk assessment in ecotoxicology. For many years, the reaction layer concept has been used fruitfully due to its simplicity for understanding and making predictions on diffusion/reaction processes. Until now, it has been applied mainly to solutions containing one ligand. Here, we reconsider the fundamentals of this approach and extend it to multiligand systems. It is shown that each metal complex has its own reaction layer (so-called composite reaction layer), which results from the interplay of this particular complex with all the other complexes. Moreover, it is shown that the overall metal flux can be computed by assuming the existence of one single fictitious equivalent reaction layer thickness for the whole of the complexes. This equivalent reaction layer is a mathematical combination of all the composite reaction layers. Simple analytical equations are obtained, which make it possible to readily interpret the role of the various types of metal species in a mixture. The revisited reaction layer approach, denoted as the reaction layer approximation (RLA), is validated by comparing the total metal flux, the individual fluxes of each metal species, and their concentration profiles computed by the RLA with those obtained by a rigorous mathematical approach. The examples of Pb(II) in a modified Aquil medium and of Cu(II) in solutions of nitrilotriacetic acid and *N*-(2-carboxyphenyl)glycine are treated in detail. In particular, an original result is obtained with the Cu/NTA/*N*-(2-carboxyphenyl)glycine system, namely an unexpected flux enhancement is observed, which is specific to solutions with ligand mixtures. The corresponding physicochemical mechanism is not readily understood by the rigorous mathematical (either numerical or analytical) solutions due to their involved combination of parameters. On the other hand, we show that, due to the simplicity of the RLA concept, the RLA facilitates elucidation of the physicochemical mechanism underlying complicated processes.

1. Introduction

Compared to metal speciation at equilibrium (i.e., thermodynamic metal species distribution), dynamic metal speciation (i.e., evaluation of the contribution of each metal species to the overall metal flux at a consuming interface) is a new field of major importance in ecotoxicology.[1−4] Flux computations at consuming interfaces, such as microoganisms[4] or bioanalogical sensors, e.g., based on permeation liquid membrane (PLM),[1,5] voltammetry,[1,5] or diffusive gradients in thin films (DGT),[6] are fundamental for understanding metal bioavailability and making predictions on dynamic risk assessment. Theories have been developed and experimentally validated a long time ago for solutions with only one ligand,[7−9] and the concept of lability was established on this basis. Only recently have rigorous mathematical approaches been derived to solve the diffusion/reaction processes at a consuming interface for multiligand systems, with either a rigorous analytical solution[10,11] or a numerical lattice Boltzmann method.[12,13] However, due to the intricate involvement of many parameters in these two computation methods[10−13] and in spite of their success in computing the total metal flux and the individual fluxes due to each metal complex, these mathematical approaches are not sufficient to understand the underlying physicochemical processes in complicated natural or biological mixtures. In particular, they cannot be used to easily predict conditions under which a metal flux might be drastically changed.

On the other hand, the simplicity of the reaction layer concept[7,14−18] more readily enables the understanding of the physicochemical mechanism of diffusion/reaction processes. It was first proposed by Brdička and Wiesner[15,19,20] when they studied the kinetic contribution of a dissociating complex ML, formed between a metal M and a ligand L, to the reduction current of M in polarography. They defined what we shall call a conventional reaction layer. Its thickness, μ (Figure 1), is expressed by $\mu = \sqrt{D_M \tau}$, where D_M is the diffusion coefficient of free metal ion and τ is its lifetime in the solution layer $0 \leq x \leq \mu$. It may be related to the association rate constant, k_a, of the reaction $M + L \rightleftharpoons ML$ via the relationship $\tau = 1/k_a[L]$:[20]

$$\mu = \sqrt{D_M/k_a[L]} \tag{1}$$

with [L] being the ligand concentration. The contribution of the complex, ML, to the total flux is only due to its dissociation inside the reaction layer. In this layer, however, the elimination of ML is slow compared to its input by diffusion from the external solution. Thus, a constant concentration of ML is assumed to exist between $x = 0$ and $x = \mu$ (Figure 1); outside this layer, steady-state concentration gradients of M and ML are formed by diffusion, and the equilibrium between M and

* Corresponding author. Telephone: ++41 22 379 6408. E-mail: Jacques.Buffle@unige.ch.

§ Present address: Department of Chemistry, University of Montreal, C. P. 6128, Succursale Centre-Ville, Montreal (QC), Canada, H3C 3J7.

10.1021/jp811429e CCC: $40.75
Published on Web 05/21/2009

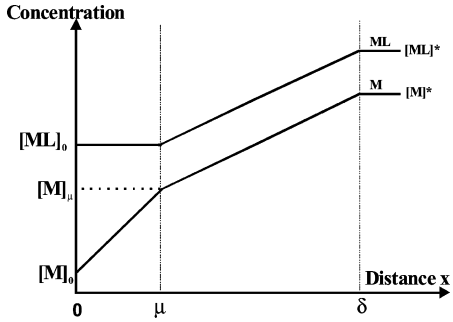

Figure 1. Schematic concentration profiles of M and ML in a solution containing a metal, M, one ligand, L, and one complex, ML where μ is the conventional reaction layer thickness and δ is the diffusion layer thickness.

ML is maintained. At a planar consuming surface, the purely kinetic metal flux, J_{kin}, can be expressed[7] (Figure 1) either by the diffusion of free M inside the reaction layer,

$$J_{kin} = D_M\left(\frac{d[M]}{dx}\right)_{x=0} \quad (2)$$

or by the chemical dissociation of ML inside this layer,

$$J_{kin} = k_d[ML]_{x=0}\mu \quad (3)$$

where k_d is the dissociation rate constant of ML.

The above explanations and Figure 1 show that, in a solution containing one ligand, the physicochemical processes leading to the metal flux can be readily understood by this simple reaction layer concept, called the reaction layer approximation (RLA). Buffle et al.[21] have used this concept to develop the corresponding mathematical formalism required to compute the metal flux at a planar or spherical consuming interface in a multiligand solution. The reaction layer thickness, μ_j, of the complex M^jL formed with the ligand ^jL, is computed by eq 1. As discussed in ref 21, this latter approach provides good results compared to rigorous mathematical computations[10] under many conditions, particularly when the kinetic properties of the various complexes are very different, i.e., when they behave independently from each other. However, the RLA based on the conventional reaction layers defined in eq 1 fails to provide good results in particular when (a) the degree of complexation of the metal is low and its diffusion coefficient is very small compared to that of the free metal ion, even in a system with only one ligand, or (b) the number of ligands is large and the association rate constants of their complexes are close to each other. For case (a), the dissociation rate is not considered in computation of the conventional reaction layer thickness (eq 1), while it should be taken into account under more general conditions.[22] For case (b), the effect of the interplay among the various complexes in the ligand mixture is neglected. Thus, in order to adapt the RLA formalism developed in ref 21 to any mixture of ligands, rigorous expressions of the reaction layer thicknesses, which overcome the aforementioned pitfalls, should replace eq 1.

In this paper, we derive rigorous analytical expressions of the reaction layer thicknesses in ligand mixtures. In addition, it is shown that the total flux can be simply computed via a single fictitious "equivalent" reaction layer thickness for the whole of the complexes. It is shown that this approach to flux computation may be very useful in complicated mixtures, in particular (i) to understand the role in the key physicochemical factors on the overall metal flux and/or (ii) to perform quick flux computations under conditions where a rigorous iterative numerical approach (e.g., using the computer code MHEDYN; see below) is very time consuming. The RLA is also a useful alternative when a rigorous analytical approach (as with the code FLUXY-RS; see below) is not possible due to the presence of successive complexes. Below, the results of metal fluxes at a planar surface behaving as a perfect sink are compared to those obtained by rigorous computations performed with the above codes.[10−13] Two environmentally relevant examples are used: (i) Pb(II) in an algal culture medium (containing 13 ligands and about 25 complexes) and (ii) Cu(II) solutions containing nitrilotriacetic acid (NTA) and *N*-(2-carboxyphenyl)glycine. In the latter case, both the RLA and rigorous computations show that an unexpected and significant flux enhancement can occur due to the presence of more than one ligand. It is used here as an example to show that the RLA is very powerful to understand the physicochemical causes of this effect, in spite of the intricate relationship between the various parameters.

2. Theory

2.1. Composite Reaction Layers in Multiligand Systems.

2.1.1. Basic Equations and Assumptions. Let us assume that the system includes n_l ligands and ^jm successive complexation reactions for each type of ligand, with $j = 1,..., n_l$. We consider a set of parallel and successive chemical reactions in solution of the following kind:

$$M^jL_{i-1} + {}^jL \underset{{}^jk_{di}}{\overset{{}^jk_{ai}}{\rightleftharpoons}} M^jL_i \qquad i = 1, \dots, {}^jm \quad (4)$$

where index i represents the stoichiometric number of ^jL in the successive complex, M^jL_i, and the superscript j is linked to the nature of the ligand. The chemical rate associated with each complex is given by

$${}^jr_i = -{}^jk_{ai}[M^jL_{i-1}][{}^jL] + {}^jk_{di}[M^jL_i] \qquad i = 1, \dots, {}^jm \quad (5)$$

where $^jk_{ai}$ and $^jk_{di}$ are the association and dissociation rate constants corresponding to the reaction 4, respectively. They are related to the equilibrium constants of the corresponding reaction, ^jK_i:

$${}^jK_i = \frac{{}^jk_{ai}}{{}^jk_{di}} = \frac{[M^jL_i]^*}{[M^jL_{i-1}]^*[{}^jL]^*} \qquad i = 1, \dots, {}^jm \quad (6)$$

where [X]* is the bulk concentration of X.

All the metal species diffuse within the solution domain by following the usual set of diffusion/reaction equations:

$$\frac{\partial[M]}{\partial t} = D_M\nabla^2[M] + \sum_{j=1}^{n_l} {}^jr_1 \quad (7)$$

$$\frac{\partial[M^jL_i]}{\partial t} = D_{M^jL_i}\nabla^2[M^jL_i] - {}^jr_1 + {}^jr_{i+1} \qquad j = 1, \dots, n_l, i = 1, \dots, {}^jm - 1 \quad (8)$$

$$\frac{\partial[M^jL_s]}{\partial t} = D_{M^jL_s}\nabla^2[M^jL_s] - {}^jr_s \qquad j = 1, \dots, n_l, \; s = {}^jm \quad (9)$$

The following assumptions/simplifications are used herein:

(a) All ligands are in excess with respect to the metal concentration, so that $[^jL] = [^jL]^* \; \forall \; j$.

(b) At $t \leq 0$, the solution is homogeneous, i.e., the concentration of any species X at the interface is the same as that in the bulk solution: [X] = [X]*.

(c) The successive complexes, M^jL_i ($i > 1$), are in equilibrium with each other and with M^jL. The corresponding justification has been discussed in ref 23: for successive complexes, often ${}^jk_{a(i+1)} > {}^jk_{ai}$ and ${}^jK_i > {}^jK_{i+1}$, so that ${}^jk_{d(i+1)} > {}^jk_{di}$. This implies that the rate-limiting step is the interchange between M and M^jL, while all the successive complexes are at equilibrium with each other. A systematic evaluation of this assumption[24] has shown that it is applicable in many cases.

(d) The system is at steady state. By also considering the above assumption (successive complexes at equilibrium), we can sum eqs 8 and 9 from $i = 1$ to ${}^jm$ to get

$$D_{M^jL_1}\nabla^2\left([M^jL_1]\frac{1}{D_{M^jL_1}{}^j\beta_1}\sum_{i=1}^{{}^jm} D_{M^jL_i}{}^j\beta_i[{}^jL]^{i-1}\right) - {}^jr_1 = 0 \qquad j = 1, \ldots, n_l \quad (10)$$

where ${}^j\beta_i$ is the cumulative stability constant of the complex M^jL_i.

(e) The reaction layer thicknesses are derived below from the steady-state fluxes at the following boundary conditions.

(i) At $x = 0$, the interface is supposed to be planar and behave as a perfect sink for M. This makes it possible to discuss the processes occurring in the solution side of the interface, irrespective of the nature of the processes of metal transfer occurring on the other side (e.g., membrane or sensor), thus simplifying the discussion. Anyway, under the conditions used here (excess of ligand), the resistance due to diffusion and reaction of the various species in solution and, thus, the expressions for the reaction layer thicknesses are not influenced by the boundary conditions. It is also assumed that, at $x = 0$, only M passes through the interface, whereas all the M^jL_i complexes are excluded (e.g., Figure 1 or 4). This is justified by the fact that most environmental ligands are hydrophilic and their complexes do not pass through plasma membranes.[24] The corresponding boundary conditions are

$$\text{at } x = 0: \qquad [M] = 0, \frac{d[M^jL_i]}{dx} = 0 \qquad j = 1, \ldots, n_l, i = 1, \ldots, {}^jm \quad (11)$$

(ii) A well-defined limit, at $x = \delta$ (Figures 1 and 2), exists between the diffusion layer and the bulk solution. The corresponding boundary conditions are

$$\text{at } x \geq \delta \quad [M] = [M]^*, [M^jL_i] = [M^jL_i]^* \qquad j = 1, \ldots, n_l, i = 1, \ldots, {}^jm \quad (12)$$

In the following, δ is assumed to be independent of metal speciation, a condition often used in such calculations (e.g., see refs 10 and 23). Rigorously, the value of δ at steady state may depend on the diffusion coefficient and chemical kinetics of the various metal species and, thus, it may vary when metal speciation changes. Experimentally, δ is often fixed by the hydrodynamic conditions (e.g, at a rotating voltametric electrode) or the geometry of the device (e.g., the gel thickness in DGT). Thus, a value of δ independent of metal speciation can be obtained either by correctly adjusting the hydrodynamic conditions or by using appropriate geometric conditions (e.g., sufficiently thick gels in DGT experiments). In practice, assuming the value of δ to be independent of speciation is often a good approximation.

In order to work with dimensionless parameters, we define below the normalized diffusion coefficients and concentrations:

$${}^j\varepsilon_i = \frac{D_{M^jL_i}}{D_M} \qquad j = 1, \ldots, n_l, i = 1, \ldots, {}^jm \quad (13)$$

$$\theta = \frac{[M]}{[M]^*} \quad (14)$$

$${}^j\psi_i = \frac{[M^jL_i]}{[M^jL_i]^*} \qquad j = 1, \ldots, n_l, i = 1, \ldots, {}^jm \quad (15)$$

Note that since there is an excess of ligand ($[{}^jL] = [{}^jL]^*$ at any distance, x), when M and M^jL_i are in equilibrium inside the diffusion layer, the relation ${}^jK_i[{}^jL]^i = [M^jL_i]/[M] = [M^jL_i]^*/[M]^*$ holds, so that at equilibrium $\theta = {}^j\psi_i$. This relationship applies in particular to all segments (numbers 3 to 6−7) of the bold, broken curve in Figure 2.

2.1.2. Derivation of the Composite Reaction Layer, $\bar{\lambda}_{n_l}$. By using eqs 14 and 15, eqs 7 and 10 can be rewritten as follows:

$$\frac{d^2\theta}{dx^2} + \sum_{j=1}^{n_l}\left(\frac{{}^jk_{a1}[{}^jL]}{D_M}{}^j\psi_1 - \frac{{}^jk_{a1}[{}^jL]}{D_M}\theta\right) = 0 \quad (16)$$

$$\frac{d^2\left({}^j\psi_1\left(\frac{1}{D_{M^jL_1}{}^j\beta_1}\sum_{i=1}^{{}^jm} D_{M^jL_i}{}^j\beta_i[{}^jL]^{i-1}\right)\right)}{dx^2} + \frac{{}^jk_{d1}}{D_{M^jL_1}}{}^j\psi_1 - \frac{{}^jk_{d1}}{D_{M^jL_1}}\theta = 0 \qquad j = 1, \ldots, n_l \quad (17)$$

Below, we assume that the order 1 to n_l also corresponds to the increasing order of the reaction layer thicknesses of the complexes M^jL (as shown in Figure 2). By multiplying the left- and right-hand sides of eq 17 by ${}^j\varepsilon_1{}^j\beta_1[{}^jL]$ and rearranging with ${}^jk_{a1}[{}^jL] = {}^jk_{d1}{}^j\beta_1[{}^jL]$, one obtains

$$\left(\sum_{i=1}^{{}^jm}{}^j\varepsilon_i{}^j\beta_i[{}^jL]^i\right)\frac{d^2({}^j\psi_1)}{dx^2} + \frac{{}^jk_{a1}[{}^jL]}{D_M}{}^j\psi_1 - \frac{{}^jk_{a1}[{}^jL]}{D_M}\theta = 0 \qquad j = 1, \ldots, n_l \quad (18)$$

By summing eqs 16 and 18, the kinetic terms cancel out and we get

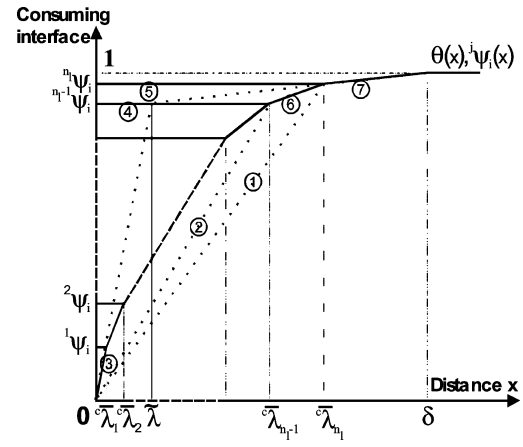

Figure 2. Schematic representation of normalized concentration profiles of M and its complexes in a mixure with n_l ligands where θ is the normalized concentration of free M, ${}^j\psi_i$ is the normalized concentration of the j^{th} set of complexes M^jL_i ($i = 1$ to ${}^jm$; see text for details), ${}^c\bar{\lambda}_j$ is the effective (corrected) composite reaction layer thickness (eqs 32 and 34), $\tilde{\lambda}$ is the equivalent reaction layer thickness (eq 40), and δ is the diffusion layer thickness. Bold lines are normalized concentration profiles by the RLA. Dotted lines: see text.

$$\frac{d^2(\theta + \sum_{j=1}^{n_l} {}^j\psi_1 \sum_{i=1}^{{}^jm} {}^j\varepsilon_i^j \beta_i [{}^jL]^i)}{dx^2} = 0 \tag{19}$$

With the normalized variables, the boundary conditions (eqs 11 and 12) now read

$$\text{At } x = 0,\ \theta = 0 \text{ and } \frac{d^j\psi_i}{dx} = 0 \qquad i = 1, ..., {}^jm, \qquad j = 1, ..., n_l \tag{20}$$

$$\text{At } x \geq \delta,\ \theta = 1 \text{ and } {}^j\psi_i = 1 \qquad i = 1, ..., {}^jm, \qquad j = 1, ..., n_l \tag{21}$$

By integrating eq 19 with these boundary conditions, we obtain

$$\theta + \sum_{j=1}^{n_l} {}^j\psi_1 \sum_{i=1}^{{}^jm} {}^j\varepsilon_i^j \beta_i [{}^jL]^i = (x - \delta)\left(\frac{d\theta}{dx}\right)_{x=0} + 1 + \sum_{j=1}^{n_l} \sum_{i=1}^{{}^jm} {}^j\varepsilon_i^j \beta_i [{}^jL]^i \qquad \text{for } 0 < x < \delta \tag{22a}$$

and

$$\theta + \sum_{j=1}^{n_l} {}^j\psi_1 \sum_{i=1}^{{}^jm} {}^j\varepsilon_i^j \beta_i [{}^jL]^i = 1 + \sum_{j=1}^{n_l} \sum_{i=1}^{{}^jm} {}^j\varepsilon_i^j \beta_i [{}^jL]^i \qquad \text{for } x \geq \delta \tag{22b}$$

Now let us derive the expression for the largest reaction layer thickness, denoted as $\bar{\lambda}_{n_l}$ in Figure 2. In the following, the symbol, λ, is used for the general expression of the reaction layer thickness in order to discriminate it from the conventional expression of the reaction layer thickness, μ (compare eqs 1 and 25). The latter, derived by Koryta and Koutecky, is well known in the literature, but only valid for solutions containing a single ligand forming a strong and quickly diffusing metal complex. The expressions of λ, below, are applicable to complexes of any strength and mobility in mixtures of ligands. As discussed in ref 10, the complex with the largest reaction layer thickness (here the set of $M^{n_l}L_i$ complexes) also has the slowest chemical kinetics. So in the RLA, in comparison with this complex, all other complexes, M^jL_i ($j < n_l$), must be assumed to be at equilibrium with M and each other. This is a basic assumption for the definition of the reaction layer, $\bar{\lambda}_{n_l}$, in the RLA. It implies that

$$\theta = {}^j\psi_i \qquad j < n_l \qquad i = 1, ..., {}^jm \tag{23}$$

So in the RLA, the boundary condition at $x = 0$ (eq 20) is now changed into

$$\theta = {}^j\psi_i = 0 \quad \text{and} \quad \frac{d^{n_l}\psi_i}{dx} = 0 \qquad i = 1, ..., {}^jm, \qquad j = 1, ..., n_l - 1 \tag{20a}$$

and accordingly, eq 22a (for $0 < x < \delta$) is also changed into

$$\theta + \sum_{j=1}^{n_l} {}^j\psi_1 \sum_{i=1}^{{}^jm} {}^j\varepsilon_i^j \beta_i [{}^jL]^i = (x - \delta)(1 + \sum_{j=1}^{n_l - 1} \sum_{i=1}^{{}^jm} {}^j\varepsilon_i^j \beta_i [{}^jL]^i)\left(\frac{d\theta}{dx}\right)_{x=0} + 1 + \sum_{j=1}^{n_l} \sum_{i=1}^{{}^jm} {}^j\varepsilon_i^j \beta_i [{}^jL]^i \tag{22c}$$

By combining eqs 16, 17, 22c, and 23 to eliminate ${}^{n_l}\psi_1$, we get

$$\frac{d^2\left[\left(1 + \sum_{j=1}^{n_l - 1} \sum_{i=1}^{{}^jm} {}^j\varepsilon_i^j \beta_i [{}^jL]^i\right)\theta\right]}{dx^2} - \frac{\dfrac{{}^{n_l}k_{a1}[{}^{n_l}L]}{1 + \sum_{j=1}^{n_l - 1} \sum_{i=1}^{{}^jm} {}^j\varepsilon_i^j \beta_i [{}^jL]^i} + \dfrac{{}^{n_l}k_{d1}}{\frac{1}{{}^{n_l}\beta_1} \sum_{i=1}^{{}^jm} {}^{n_l}\varepsilon_i^{n_l} \beta_i [{}^{n_l}L]^{i-1}}}{D_M} \left[\left(1 + \sum_{j=1}^{n_l - 1} \sum_{i=1}^{{}^jm} {}^j\varepsilon_i^j \beta_i [{}^jL]^i\right)\theta\right] +$$

$$\frac{{}^{n_l}k_{a1}[{}^{n_l}L]}{D_M \sum_{i=1}^{{}^jm} {}^{n_l}\varepsilon_i^{n_l} \beta_i [{}^{n_l}L]^i}\left(1 + \sum_{j=1}^{n_l - 1} \sum_{i=1}^{{}^jm} {}^j\varepsilon_i^j \beta_i [{}^jL]^i\right)\left(\frac{d\theta}{dx}\right)_{x=0}(x - \delta) + \frac{{}^{n_l}k_{a1}[{}^{n_l}L]}{D_M \sum_{i=1}^{{}^jm} {}^{n_l}\varepsilon_i^{n_l} \beta_i [{}^{n_l}L]^i}\left(1 + \sum_{j=1}^{n_l} \sum_{i=1}^{{}^jm} {}^j\varepsilon_i^j \beta_i [{}^jL]^i\right) = 0 \tag{24}$$

The combination parameter, λ_{n_l}, appears as a physically meaningful parameter:

$$\bar{\lambda}_{n_l} = \sqrt{\frac{D_M}{\dfrac{{}^{n_l}k_{a1}[{}^{n_l}L]}{1 + \sum_{j=1}^{n_l - 1} \sum_{i=1}^{{}^jm} {}^j\varepsilon_i^j \beta_i [{}^jL]^i} + \dfrac{{}^{n_l}k_{d1}}{\frac{1}{{}^{n_l}\beta_1} \sum_{i=1}^{{}^jm} {}^{n_l}\varepsilon_i^{n_l} \beta_i [{}^{n_l}L]^{i-1}}}} \tag{25}$$

It is the reaction layer thickness of the set of complexes $M^{n_l}L_i$ under a semi-infinite diffusion condition. Thereafter, it is denoted as the composite reaction layer thickness of $M^{n_l}L_i$ because it is influenced by (i) all the successive complexes $M^{n_l}L_i$ and (ii) all the complexes M^jL_i ($1 \leq j < n_l$; $i \geq 1$). Equation 25 is clearly a more general expression of the reaction layer than that obtained in a solution containing a single ligand and a single complex, i.e.:[22]

$$\lambda = \sqrt{\frac{D_M}{k_a[L] + k_d/\varepsilon}}$$

This latter equation, in turn, is a more general expression than the conventional reaction layer thickness (eq 1), which is obtained when $k_d/\varepsilon \ll k_a[L]$ (i.e., $\varepsilon K[L] \gg 1$).

In eq 25, we define the dynamic degree of complexation, α'_k as

$$\alpha'_k = 1 + \sum_{j=1}^{k} \sum_{i=1}^{{}^{j}m} {}^{j}\varepsilon_i^{\,j}\beta_i[{}^{j}L]^i \tag{26}$$

and

$$q_j = \frac{1}{{}^{j}\beta_1} \sum_{i=1}^{{}^{j}m} {}^{j}\varepsilon_i^{\,j}\beta_i[{}^{j}L]^{i-1} \tag{27}$$

By integrating eq 24 with eqs 25−27 and the boundary conditions (20a) and (21), we get

$$\alpha'_{n_l-1}\theta = {}^{n_l}C_1 \exp(-x/\bar{\lambda}_{n_l}) + {}^{n_l}C_2 \exp(x/\bar{\lambda}_{n_l}) + \frac{\alpha'^2_{n_l-1}\left(\frac{d\theta}{dx}\right)_{x=0} x}{\alpha'_{n_l}} + \alpha'_{n_l-1} - \frac{\alpha'^2_{n_l-1}\left(\frac{d\theta}{dx}\right)_{x=0}\delta}{\alpha'_{n_l}} \tag{28}$$

where ${}^{n_l}C_1$ and ${}^{n_l}C_2$ are constants given by

$${}^{n_l}C_1 = \frac{\left(\alpha'_{n_l-1} - \frac{\alpha'^2_{n_l-1}}{\alpha'_{n_l}}\left(\frac{d\theta}{dx}\right)_{x=0}\delta\right)\exp(2\delta/\bar{\lambda}_{n_l})}{1 - \exp(2\delta/\bar{\lambda}_{n_l})} \tag{29}$$

$${}^{n_l}C_2 = \frac{\frac{\alpha'^2_{n_l-1}}{\alpha'_{n_l}}\left(\frac{d\theta}{dx}\right)_{x=0}\delta - \alpha'_{n_l-1}}{1 - \exp(2\delta/\bar{\lambda}_{n_l})} \tag{30}$$

The flux, $J_{n_l} = D_M\alpha'_{n_l-1}(d\theta/dx)_{x=0}$, is then obtained as:

$$J_{n_l} = D_M[M]^*\left[\frac{\delta}{\alpha'_{n_l}} + \frac{\bar{\lambda}_{n_l}(\alpha'_{n_l} - \alpha'_{n_l-1})}{\alpha'_{n_l}\alpha'_{n_l-1}}\tanh\left(\frac{\delta}{\bar{\lambda}_{n_l}}\right)\right]^{-1} \tag{31}$$

J_{n_l} is the total flux under the basic assumption discussed above (leading in particular to eq 23). Its value is not the exact solution. For instance, with the present assumption, $(d\theta/dx)_{x=0}$ is the slope of line 1, while the correct total flux should be given by the slope of line 3 (Figure 2). In other words, in our approximation, the real concentration profile of M (bold lines 3−6) is approximated by line 1. Equation 31, however, is useful for two reasons: (i) it has the same form as the flux equation in a solution containing only one ligand and one complex,[21,22] which confirms its validity, and (ii) it shows that, as for the case of a single ligand, the reaction layer thickness (here $\bar{\lambda}_{n_l}$) should be corrected by a term $\tanh(\delta/\bar{\lambda}_{n_l})$. Thus, the effective reaction layer thickness is

$${}^{c}\bar{\lambda}_{n_l} = \bar{\lambda}_{n_l}\tanh\left(\frac{\delta}{\bar{\lambda}_{n_l}}\right) \tag{32}$$

which takes into account the fact that ${}^{c}\bar{\lambda}_{n_l}$ cannot be larger than δ. Indeed, when $\delta \to \infty$, $\tanh(\delta/\bar{\lambda}_{n_l}) = 1$ and, thus, ${}^{c}\bar{\lambda}_{n_l} = \bar{\lambda}_{n_l}$ (semi-infinite diffusion condition). When $\delta/\bar{\lambda}_{n_l} \to 0$, $\tanh(\delta/\bar{\lambda}_{n_l}) \to \delta/\bar{\lambda}_{n_l}$ and ${}^{c}\bar{\lambda}_{n_l} = \delta$.

2.1.3. Composite Reaction Layer, $\bar{\lambda}_j$. The expressions of the composite reaction layer thickness, λ_{n_l-1}, of the set of complexes $M^{n_l-1}L_i$ ($i = 1$ to ${}^{n_l-1}m$) can be found by following the same procedure (Supporting Information, Section 1) as that used in Section 2.1.2. The general equation for the composite reaction layer thickness, $\bar{\lambda}_j$, of any set of complexes M^jL_i ($i = 1$ to ${}^{j}m$) is deduced similarly:

$$\bar{\lambda}_j = \sqrt{\frac{D_M}{\sum_{i=j}^{n_l} {}^{i}k_{a1}[{}^{i}L]/\alpha'_{j-1} + {}^{j}k_{d1}/q_j}} \qquad j = 1, \ldots, n_l \tag{33}$$

with

$$\alpha'_j = 1 + \sum_{i=1}^{j} \sum_{k=1}^{{}^{j}m} {}^{i}\varepsilon_k^{\,i}\beta_k[{}^{i}L]^k \quad \text{and } \alpha'_0 = 1, \quad \text{and}$$

$$q_j = \frac{1}{{}^{j}\beta_1} \sum_{k=1}^{{}^{j}m} {}^{j}\varepsilon_k^{\,j}\beta_k[{}^{j}L]^{k-1}$$

In Supporting Information, eq S13 shows that the effective reaction layer, ${}^{c}\bar{\lambda}_j$, can be obtained from ${}^{c}\bar{\lambda}_{j+1}$(eq 34) and $\bar{\lambda}_j$ (eq 33):

$${}^{c}\bar{\lambda}_j = \bar{\lambda}_j \tanh\left(\frac{{}^{c}\bar{\lambda}_{j+1}}{\bar{\lambda}_j}\right) \qquad j = 1, \ldots, n_1 - 1 \tag{34}$$

2.2. Metal Flux and Equivalent Reaction Layer $\tilde{\lambda}$. In the conventional reaction layer concept with one single ligand,[7] the metal flux is obtained by (Figure 1)

$$J = D_M\left(\frac{d[M]}{dx}\right)_{x=0} = D_M\frac{[M]_\mu}{\mu} \tag{35}$$

where $[M]_\mu$ is the concentration of the free metal ion M at the boundary μ. By analogy, in the RLA with a multiligand mixture, the total metal flux is defined by eq 36:

$$J = \frac{D_M[M]_{\tilde{\lambda}}}{\tilde{\lambda}} \tag{36}$$

where $\tilde{\lambda}$ is a fictitious "equivalent" reaction layer, applicable to the whole of the complexes. $\tilde{\lambda}$ and $[M]_{\tilde{\lambda}}$ are related to the set of the above composite reaction layer thicknesses, as follows. The expression of the permeability, $P = J/[M]^*$ (units = m/s), for a multiligand system has been derived in ref 21 based on the RLA and using the expressions for the conventional reaction layer thickness, μ (eq 1) for all complexes.

$$P = \left[\frac{\delta}{D_M\alpha'_t} + \sum_{j=1}^{n_l}\mu_j\left(\frac{1}{D_M\alpha'_{j-1}} - \frac{1}{D_M\alpha'_j}\right)\right]^{-1} \tag{37}$$

where

$$\alpha'_t = \alpha'_{n_l} = 1 + \sum_{j=1}^{n_l} \sum_{k=1}^{{}^{j}m} {}^{j}\varepsilon_k^{\,i}\beta_k[{}^{j}L]^k$$

P reflects the easiness of transferring M through the whole interface, irrespective of the concentration of M. Expressing the μ_j by eq 1 in eq 37 implies that all complexes are independent of each other (see Introduction). For interrelated complexes, the μ_j's should be replaced by the effective composite reaction layer thickness, ${}^{c}\bar{\lambda}_j$, described above. By doing so and re-arranging eq 37, one gets

$$P = \left[\frac{\delta}{D_M \alpha'_t} + \frac{\alpha'_t - 1}{D_M \alpha'_t}\left[\frac{\alpha'_t}{\alpha'_t - 1}\sum_{j=1}^{n_l} {}^c\bar{\lambda}_j\left(\frac{1}{\alpha'_{j-1}} - \frac{1}{\alpha'_j}\right)\right]\right]^{-1} \quad (38)$$

By comparing this expression with that corresponding to the flux of M in the presence of a single ligand[22]

$$P = \left[\frac{\delta}{D_M \alpha'_t} + \frac{\alpha'_t - 1}{D_M \alpha'_t} {}^c\lambda\right]^{-1} \quad (39)$$

one can define, for the whole mixture of complexes, an equivalent reaction layer thickness, $\tilde{\lambda}$, composed of the set of the above composite reaction layers, as follows:

$$\tilde{\lambda} = \frac{\alpha'_t}{\alpha'_t - 1}\sum_{j=1}^{n_l} {}^c\bar{\lambda}_j\left(\frac{1}{\alpha'_{j-1}} - \frac{1}{\alpha'_j}\right) \quad (40)$$

In summary, the metal flux in a mixture of complexes can be computed via a single (fictitious) equivalent reaction layer, $\tilde{\lambda}$, determined by the whole of the (real) composite reaction layers, which characterize each complex but are also influenced by the other complexes (see also definitions and symbols, and section 4.1). In practice, to compute $\tilde{\lambda}$ in a mixture of complexes, the terms ${}^j\kappa = {}^jk_{d1}/q_j$ (eq 33) are first computed and sorted in decreasing order. Indeed, it has been shown, for multiligand systems in the absence of successive complexes,[10] that the reaction layer thicknesses of the complexes M^jL decrease with ${}^jk_d/{}^j\varepsilon$; ${}^jk_{d1}/q_j$ is equivalent to this parameter. Once the ligands are ordered, the corresponding effective composite reaction layer thicknesses can be computed by eqs 32−34. The value for $\tilde{\lambda}$ is then obtained by eq 40.

The total flux is then readily computed based on this fictitious single equivalent reaction layer. Analogous to the single ligand case, all metal species are assumed to be at equilibrium with each other between the bulk solution ($x = \delta$) and the boundary of the equivalent reaction layer ($x = \tilde{\lambda}$) and the metal flux is diffusion controlled:

$$J = \frac{D_M \alpha'_t([M]^* - [M]_{\tilde{\lambda}})}{\delta - \tilde{\lambda}} \quad (41)$$

Inside the equivalent reaction layer, J is given by the diffusion of free M only (eq 36) (Figure 1). At a steady state, due to the continuity of fluxes, eqs 36 and 41 are equal. In addition, when all complexes are fully labile, J is equal to the total maximum flux, J_{lab}, given by eq 42.

$$J_{lab} = \frac{D_M \alpha'_t [M]^*}{\delta} \quad (42)$$

Combining eqs 36, 41, and 42 leads to eq 43 for the flux, J:

$$J = \frac{J_{lab}}{1 + \frac{\tilde{\lambda}}{\delta}(\alpha'_t - 1)} = \frac{D_M \alpha'_t [M]^*}{\delta + \tilde{\lambda}(\alpha'_t - 1)} \quad (43)$$

On the other hand, by combining eqs 36, 40, and 41, it is also possible to compute the values of $[M]_{\tilde{\lambda}}$. Equation 43, combined with eqs 40 and 34, is a very simple and useful equation, applicable to quite complicated mixtures of ligands. It does not even require finding the eigenvalues of matrices, as in ref 10, and it is applicable to successive complexes provided their kinetics are faster than those of the corresponding M^jL complex, which is often the case as discussed in refs 23 and 24. It enables simple predictions to be made and facilitates understanding of the physical role of factors controlling J because the kinetic and thermodynamic parameters are partly separated in the terms $\tilde{\lambda}$ and α'_t, respectively, which are readily computed. Note that eq 43 reduces to the straightforward limiting cases: when all complexes are labile, $\tilde{\lambda}$ tends to 0 (all chemical rate constants are very large) and $J \sim J_{lab}$; when all complexes are inert $\tilde{\lambda}/\delta \rightarrow 1$ and $\tilde{\lambda}(\alpha'_t - 1)/\delta \rightarrow \alpha'_t - 1$, then $J = D_M[M]^*/\delta$, which corresponds to the metal flux in a solution of inert complexes; the fully kinetically controlled flux ($J = D_M[M]^*/\tilde{\lambda}$) is obtained when $\tilde{\lambda}\alpha'_t/\delta \gg 1$, while $\tilde{\lambda}/\delta < 1$.

TABLE 1: Species Distribution of Pb(II) in the Test Culture Medium As Determined by MINTEQ2[28,a]

Component	Pb (%)	
Free metal ion	1.665	
PbCl	6.40	11.83
$PbCl_2$	3.58	
$PbCl_3$	1.33	
$PbCl_4$	0.52	
$PbCO_3$	26.85	
PbIDA	23.25	
PbNTA	33.95	

[a] Each line gives the proportion (in %) of the most important (>0.5%) metal species with respect to the total metal concentration. $T = 25°C$, $I = 0.576$ M, and pH = 8. The values of stability constants used are those of ref 30 by using a correcting factor, $b = 0.2$, in the Davies equation. Total Pb(II) concentrations: 2×10^{-9} M.

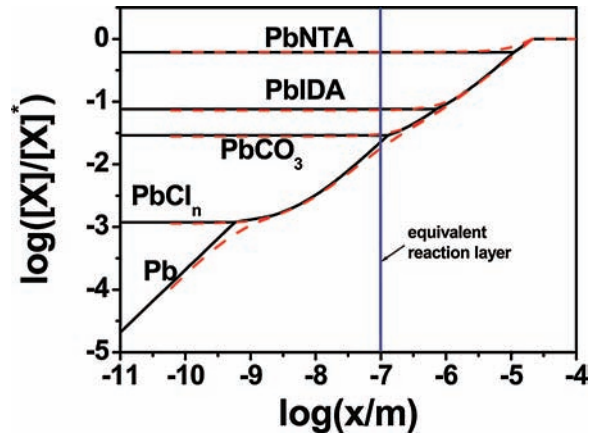

Figure 3. Normalized concentration profiles of the metal species of Pb in the modified Aquil medium (composition: see Supporting Information, Table S1). Bold black lines are curves computed by the RLA. Dotted red lines are curves obtained by rigorous method. The vertical blue line shows the equivalent reaction layer computed as mentioned in the text.

3. Computation Method

The flux and concentration profiles of Table 1 and Figure 3 are rigorously computed by using the flux computation code MHEDYN (Multispecies HEtergeneous DYNamics),[26] which is based on a Lattice-Boltzmann method for the numerical solution of the diffusion/reaction equations. It is coupled to a time-splitting technique and a grid-refinement method[12,13] in order to treat physicochemical systems with dynamic parameters varying over many orders of magnitude. Systems containing an unlimited number of ligands and complexes can be treated. The major characteristic of MHEDYN is that the contribution to metal flux and the concentration profile of any species can

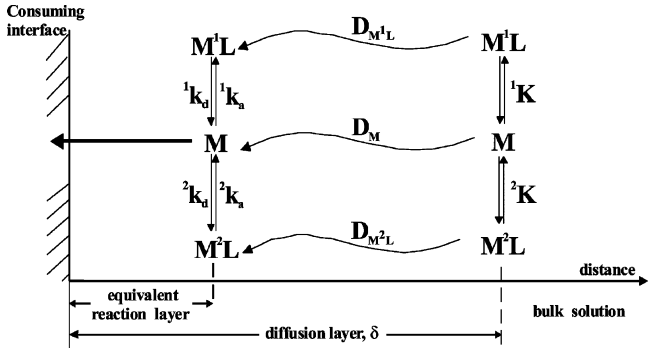

Figure 4. Schematic representation of the diffusion/reaction processes of two metal complexes near a consuming interface. D_{M^jL} and D_M are the diffusion coefficients of M^jL and free metal ion, ^jK is the complexation stability constant of M^jL, ^jk_a, ^jk_d are the formation/dissociation rate constants of M^jL, and δ is the diffusion layer thickness.

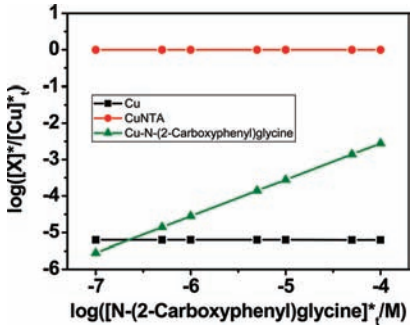

Figure 5. Cu(II) species distribution at equilibrium in a Cu(II) solution containing NTA and *N*-(2-carboxyphenyl)glycine, where X indicates Cu, Cu−NTA or Cu−*N*-(2-carboxyphenyl)glycine and $[Cu]_t$* is the total bulk Cu concentration, pH = 7, I = 0.1 M, and T = 25 °C. Computations are done with MINTEQ 2.[28]

be computed in the transient and steady-state regimes, without requirement of ligand excess compared to metal. Its major drawback is that it may be time consuming, depending on the conditions. In particular, very small grid sizes and computer time steps should be used to get precise profiles of Pb^{2+} and $PbCl_n$ in Figure 3 with MHEDYN, due to the very large rate constants of the latter (profiles in the nanometer range). So this part of the profiles of Fig 3 were computed with the rigorous analytical solutions of ref 10.

The rigorous computations of Figure 6a,b were performed by means of the code FLUXY in the computing mode RS.[21,24] The corresponding algorithm is based on the rigorous analytical solution of diffusion/reaction equations[10] with the assumptions that the ligands are in excess with respect to the metal. Computations with FLUXY are fast. FLUXY-RS, however, is not applicable in the presence of successive complexes. FLUXY-RLA must then be used. Both codes, MHEDYN and FLUXY, are available at http://www.unige.ch/cabe/dynamic.

In the two applications discussed below, metal fluxes are computed in solutions containing mixtures of ligands at planar consuming interfaces, behaving as perfect sinks for the free metal ion, i.e., the so-called maximum metal flux is computed.[24] Such conditions apply, for instance, to chemical sensors of metals (voltammetric deposition, flux at permeation liquid membrane (PLM), or diffusive gradient in thin films (DGT)), in natural waters or biological samples. The maximum metal flux is independent of the nature of the interface and the consuming process and depends only on processes occurring in solution. For more discussion, see refs 1, 4, 5, and 25.

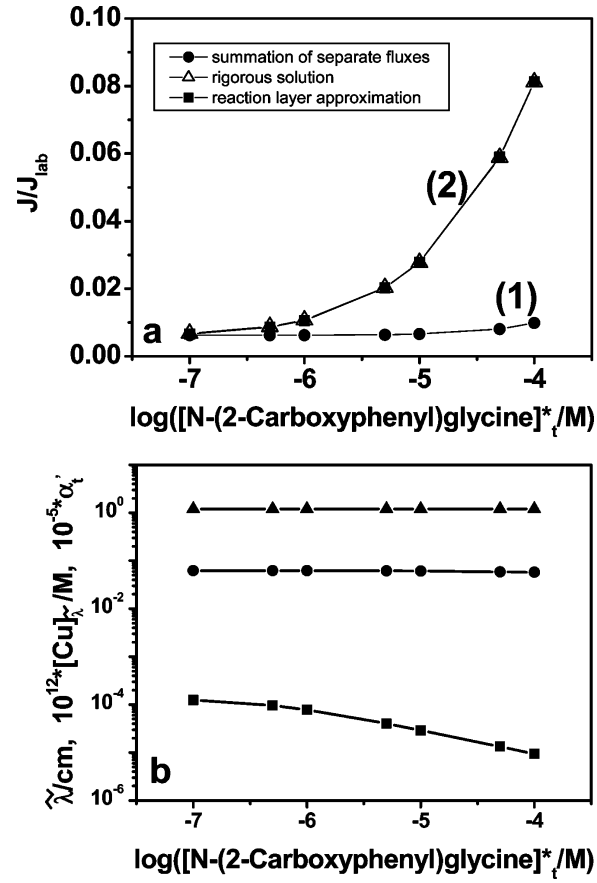

Figure 6. (a) Normalized flux of Cu, i.e., the ratio of total flux, J, to the maximum flux, which would be obtained if all complexes were fully labile, J_{lab}, as a function of the total concentration of *N*-(2-carboxyphenyl)glycine (≡^{1}L) in a solution containing Cu(II) (total bulk concentration, $[Cu]_t$*, = 10^{-8} M) and NTA (≡^{2}L; total bulk concentration, $[NTA]_t$* = 10^{-5} M) at pH = 7, I = 0.1 M, and T = 25 °C. The effective flux (curve 2) is computed by both the rigorous analytical solution (triangles) and the RLA (black squares; eq 43). Curve 1 corresponds to the flux which would be obtained if the complexes were independent of each other. (b) Changes of the equivalent reaction layer thickness, $\tilde{\lambda}$ (■), of the free Cu concentration at the boundary of $\tilde{\lambda}$ (•) and the dynamic degree of complexation, α_t' (▲), with the total bulk concentration of *N*-(2-carboxyphenyl)glycine. Other conditions see Figure 6a.

4. Applications to Environmentally Relevant Systems

4.1. Total and Individual Fluxes of Pb in Modified Aquil Medium. As a first example of application of the revisited RLA, the maximum flux of Pb(II) is computed in a culture medium of algae, containing several ligands, forming complexes with widely varying chemical kinetics and many successive complexes. A modified Aquil[27] culture medium (Supporting Information, Table S1) has been selected in which EDTA is replaced by NTA and IDA. At the chosen pH (pH = 8), ionic strength (0.576 M), and ligand concentrations, the main Pb(II) species in the bulk solution are chloro-complexes (11.8%), $PbCO_3^0$ (26.8%), Pb-IDA (23.2%), and Pb-NTA (34.0%). Table 1 provides the distribution of the most important species (see below) of Pb(II), computed by MINTEQ2.[28] It must be emphasized that, in addition to the presence of successive complexes, the rate and equilibrium constants of the whole of the complexes vary over orders of magnitudes (k_a values range from 5×10^6 to 2×10^7 m^3 mol^{-1} s^{-1}, k_d values vary from 3.95 s^{-1} to 2.29×10^9 s^{-1}, and $\log(K/M^{-1})$ spans 0.897 to 9.69 (where K is the stepwise equilibrium constant)). This system

TABLE 2: Comparison of the Total and Individual Fluxes and Degrees of Lability[10] of Pb(II) Species in the Modified Aquil Medium[a] Computed by the RLA and MHEDYN

	individual flux (mol m^{-2} s^{-1})		degree of lability	
species X	RLA	rigorous method	RLA	rigorous method
Pb	1.48×10^{-12}	1.48×10^{-12}	1	1
PbCl	6.78×10^{-12}	6.78×10^{-12}	0.999	0.998
$PbCl_2$	3.79×10^{-12}	3.79×10^{-12}	0.999	0.998
$PbCl_3$	1.40×10^{-12}	1.40×10^{-12}	0.999	0.998
$PbCl_4$	5.46×10^{-13}	5.45×10^{-13}	0.999	0.998
$PbCO_3$	2.31×10^{-11}	2.32×10^{-11}	0.971	0.972
PbIDA	1.91×10^{-11}	1.91×10^{-11}	0.924	0.927
PbNTA	9.00×10^{-12}	8.86×10^{-12}	0.387	0.380
total	6.52×10^{-11}	6.52×10^{-11}		

[a] See Supporting Information, Table S1 for full composition.

is, thus, a challenging test of the validity of the proposed equations for the RLA in ligand mixtures.

For each complex, the values of the association rate constants were computed as explained in ref 25. Their values, as well as those of the thermodynamic stability constants and diffusion coefficients, used in this paper are listed in Supporting Information, Table S2. For the successive complexes, their chemical kinetics were taken into account in the rigorous computations with MHEDYN, while all ML_i complexes ($i > 1$) were considered at equilibrium with ML in the RLA-based computations. The equilibrium species distribution was computed for all possible Pb(II) complexes with the ligands of Supporting Information, Table S1. Tables 1 and 2 only report the results for those species whose proportion is larger than 1% of the total Pb(II) and which may play a significant role in the total flux (their overall contribution to the total flux is 97.8%).

Table 2 provides the total and individual Pb(II) fluxes and the corresponding degrees of lability, ${}^j\xi$, computed by the RLA and MHEDYN. ${}^j\xi$ is defined as[10]

$$ {}^j\xi = \left(1 - \frac{[\mathrm{M}^j\mathrm{L}]^0}{[\mathrm{M}^j\mathrm{L}]^*}\right) \Big/ \left(1 - \frac{[\mathrm{M}]^0}{[\mathrm{M}]^*}\right) \tag{44} $$

where the superscript ^{0} denotes the surface concentrations of M and M^jL. In the RLA, ${}^j\xi$ and individual flux are computed by[21]

$$ {}^j\xi = \left(1 - \frac{[\mathrm{M}]_{c\bar{\lambda}_j}}{[\mathrm{M}]^*}\right) \Big/ \left(1 - \frac{[\mathrm{M}]^0}{[\mathrm{M}]^*}\right) \tag{45} $$

$$ {}^jJ = \frac{D_{\mathrm{M}j\mathrm{L}}[\mathrm{M}^j\mathrm{L}]^*}{\delta}\left(1 - \frac{[\mathrm{M}]_{c\bar{\lambda}_j}}{[\mathrm{M}]^*}\right) \tag{46} $$

where $[\mathrm{M}]_{c\bar{\lambda}_j}$ denotes the concentration of free metal ion, M, at the boundary of the composite reaction layer, ${}^c\bar{\lambda}_j$, of complex, M^jL. Table 2 shows that the results of the RLA and MHEDYN are in very good agreement. The degrees of lability computed by both methods are almost the same, and the average difference in individual fluxes is 0.27%. So under the conditions used, the RLA satisfactorily computes the fluxes in multicomponent systems, even in the presence of significant contributions of successive complexes and in a mixture of complexes with a very large range of rate and equilibrium constants (see above).

Interestingly, Figure 3 shows that the RLA also enables to generate, in a simple manner, very good approximations of concentration profiles of the various metal species in the ligand mixture. As shown in Figure 2, the normalized concentration profile of free M is the connection of a series of points (from ($x = 0$, $\psi = 0$), via ($x = {}^c\bar{\lambda}_j$, $\psi = {}^j\psi_1{}^0$) to ($x = \delta$, $\psi = 1$). The bold black lines obtained by the RLA in Figure 3 follows this strategy. Note that figure 3 is similar to Figure 2, except that the x axis is in a logarithmic scale, due to the very wide range of covered values of ${}^c\bar{\lambda}_j$. It is seen that, for all the species of Pb(II) in Aquil medium, the concentration profiles based on the ${}^c\bar{\lambda}_j$ values obtained by the RLA compare very well with those directly computed by MHEDYN or the rigorous equations of ref 10. It must be emphasized that computations with MHEDYN may take days, while those with the RLA take less than an hour.

4.2. Interpreting Unexpected Metal Flux Enhancement; The Cu/NTA/*N*-(2-Carboxyphenyl)glycine System. This section shows the capability of the RLA to interpret the physicochemical reasons of the effect of a given factor on metal flux in ligand mixtures. Let us consider a solution containing a metal ion, M, and two different ligands, ^1L and ^2L, forming the complexes M^1L and M^2L in contact with a consuming interface acting as a perfect sink for M (Figure 4). In addition, only M, and not the complexes or ligands, is consumed at the interface, as it is often the case for the uptake of metal by microorganisms.[4,9] We maintain constant the bulk concentration of one ligand (e.g., ^2L) while the bulk concentration of the other one, $[^1L]^*$, is increased in such a way that $1 \ll {}^1K[^1L]^* \ll {}^2K[^2L]^*$, which implies that $[M^1L]^* \ll [M^2L]^* \sim [M]_t^*$ where $[M]_t^*$ is the bulk total concentration of M. Since the bulk concentration of M^1L remains negligible, both $[M]^*$ and $[M^2L]^*$ are almost unchanged. Thus, an intuitive guess would suggest that the flux at the interface would also remain constant, as if the reaction $M \leftrightarrow M^1L$ would not exist. However, significant departure from this behavior may occur, as it is exemplified below.

Figure 5 shows the distribution of Cu(II) species in a mixture of NTA ($\equiv {}^2L$) and *N*-(2-carboxyphenyl)glycine ($\equiv {}^1L$) and highlights that Cu−NTA is always in large excess compared to Cu^{2+} and Cu^1L. Figure 6a shows the flux of Cu(II) computed in different ways with the parameter values given in the Supporting Information, Table S3. Curve 1 is the plot which would be obtained if the total flux was just the sum of the fluxes due to Cu, Cu^1L, and Cu^2L, assuming that they are independent of each other. Since $[Cu]^*$ and $[Cu^2L]^*$ are constant and $[Cu^1L]^*$ is negligible in the whole range of $[^1L]^*$ explored, a constant flux is then expected. Rigorous mathematical calculations,[10] however, (curve 2, triangles), which take into account the interplay between the three Cu species at the interface, show a completely different picture: (i) the real flux strongly increases with $[^1L]^*$ in spite of the negligible concentration of Cu^1L under the studied conditions, and (ii) the real flux may be an order of magnitude larger than the "expected" flux computed by assuming an independent behavior of the three species. Figure 6a also shows that the RLA (curve 2, black squares; eq 43) is in excellent agreement with rigorous calculations and is, thus, fully capable of taking into account the interplay of the various species.

The most interesting feature of the RLA (eq 43) is that it allows us to better understand the kinetic or thermodynamic effect of each ligand on the total flux. Indeed, in eqs 36 and 43 $\tilde{\lambda}$ mainly depends on the formation and dissociation rates of the complexes, while $[M]_{\tilde{\lambda}}$ (eq 36) or α_t' (eq 43) mainly depends on the thermodynamic stability of complexes (particularly with small ligands for which ${}^j\varepsilon \sim 1$); mathematically, the value of $\tilde{\lambda}$ is primarily determined by summations of ${}^jk_a[^jL]^*$ terms (eqs 33, 34 and 40), while that of α_t' results from a summation of ${}^jK[^jL]^*$ terms. Detailed analysis of such equations shows that usually in complicated mixtures, only a few ligands (a few ${}^jk_a[^jL]^*$ or a few ${}^jK[^jL]^*$ terms) play a predominant role in both $\tilde{\lambda}$ and α_t'. The key point is that the predominant terms of $\tilde{\lambda}$ and

α'_t are not necessarily due to the same ligand. Thus, increasing the concentration of one ligand may, for instance, decrease $\tilde{\lambda}$ drastically while α'_t remains approximately constant (see Figure 6b). For a kinetically controlled flux ($\tilde{\lambda}$ ($\alpha'_t - 1$) $\gg \delta$ in eq 43), the net effect will be an increase of total flux, even though no change would be expected based on the species thermodynamic distribution in the bulk solution.

This is exemplified in Figure 6b which shows the changes of α'_t, the equivalent reaction layer thickness, $\tilde{\lambda}$, and the free Cu^{2+} concentration, $[Cu]_{\tilde{\lambda}}$, at the boundary of the equivalent reaction layer with the total bulk concentration of *N*-(2-carboxyphenyl)glycine. This ligand corresponds to ligand ^1L in Figures 2 and 4, i.e., it forms a complex more labile than M^2L and, thus, tends to decrease the equivalent reaction layer thickness, $\tilde{\lambda}$, when its concentration is increased. This can be quantitatively seen from eq 47, which is obtained from eq 40, by realizing that in the present case ${}^c\bar{\lambda}_j \sim \mu_j$ (eq 1)

$$\tilde{\lambda} \approx \frac{\alpha'_t}{\alpha'_t - 1}\left[\sqrt{\frac{D_M}{{}^1k_a[{}^1L]^*}}\left(1 - \frac{1}{\alpha'_1}\right) + \sqrt{\alpha'_1}\sqrt{\frac{D_M}{{}^2k_a[{}^2L]^*}}\left(\frac{1}{\alpha'_1} - \frac{1}{\alpha'_2}\right)\right] \quad (47)$$

By taking into account that $[^2L]^*$ is constant, $1/\alpha'_1 \sim 1/{}^1K[^1L]^* \ll 1$, $1/\alpha'_2 \ll 1/\alpha'_1$ and $\alpha'_t \gg 1$, eq 47 clearly shows that $\tilde{\lambda}$ decreases with $[^1L]^*$. Simultaneously, Figure 6b also shows that, under the conditions used, α'_t and $[Cu]_{\tilde{\lambda}}$ remain almost constant. Indeed, the increase of complexation strength by ^1L is negligible compared to that due to NTA, and [Cu] is well buffered by Cu−NTA, which is largely dominant in solution. By combining this constant value of $[Cu]_{\tilde{\lambda}}$ (or α'_t) with the drastic decrease of $\tilde{\lambda}$, the concentration gradient of free copper increases at the consuming surface (Figure 2) and the flux considerably increases (eq 36). A detailed analysis of the flux enhancement process based on the RLA is given in ref 29 and is out of the scope of this paper.

Physically, the decrease of $\tilde{\lambda}$ corresponds to a decrease of lifetime, τ (see Introduction), of Cu^{2+} in the reaction layer due to the fact that by increasing $[^1L]^*$, the fraction of time spent by M, under the form M^1L, increases and, consequently, the lifetime of free M decreases (Figure 4). This occurs, even though the proportion of M^1L remains negligible compared to M^2L.

This result has important implications for the bio-uptake of metals in environmental or biological systems. Trace metals are often predominantly complexed with strong (organic) ligands forming semi- or nonlabile complexes. On the other hand, all natural media contain many inorganic (OH^-, CO_3^{2-}, Cl^-) or small organic ligands (oxalate, tartrate), which form weak, but labile complexes with those metals. It may, thus, be expected that even though such ligands may not play a major role in controlling the metal distribution in the bulk solution, they might play a significant role by increasing the bio-uptake flux of trace metals via the aforementioned mechanism.

5. Conclusions

In the revisited reaction layer approximation (the RLA), the metal flux in a ligand mixture can be computed based on a single, fictitious equivalent reaction layer, similar to the treatment used for a solution with a single ligand and the conventional reaction layer concept. It has been shown that the equivalent reaction layer thickness can be evaluated from the real composite reaction layer thicknesses corresponding to each metal complex. The composite and equivalent reaction layer thicknesses are influenced by the interplay between all the complexes at the interface. Nevertheless, the composite reaction layers correspond to physically well-defined layers of solution. This has been checked quantitatively by comparing the results of the RLA with those obtained by rigorous calculations. In particular, the total flux, individual fluxes, and concentration profiles of each metal species have been compared in the modified Aquil medium. In addition, the physicochemical mechanism of the unexpected flux enhancement observed with the Cu/NTA/*N*-(2-carboxyphenyl)glycine system is readily interpreted by the RLA. Those results show that the extension of the RLA to solutions containing mixtures of ligands is very useful not only for simple computation of metal fluxes, but also to understand the details of physicochemical processes taking place in complicated systems at the consuming interface.

Acknowledgment. J. Puy and R. M. Town are gratefully acknowledged for their useful discussions.

Appendix

Definitions and Symbols

Definitions of Reaction Layer Thicknesses

μ	$(D_M/k_a[L])^{1/2}$, conventional expression of the reaction layer thickness valid for a solution with one ligand forming a strong complex ML with $D_{ML} \sim D_M$
λ	$((D_M)/(k_a[L] + k_d/\varepsilon))^{1/2}$, general expression of the reaction layer thickness for a solution containing one ligand
$\bar{\lambda}$	composite reaction layer thickness for a given complex in the presence of several other ligands under conditions of semi-infinite diffusion (time-dependent diffusion layer thickness not imposed by geometric or hydrodynamic conditions)
${}^c\bar{\lambda}$	effective composite reaction layer thickness, as above, but under conditions where the diffusion layer thickness is imposed by external conditions and independent of time
$\tilde{\lambda}$	(fictitious) equivalent reaction layer thickness, representative of the kinetics of the whole of the metal complexes in a mixture of ligands

List of Symbols

D_M	the diffusion coefficient of free metal ion
J	the metal flux
J_{lab}	the maximum metal flux when all the complexes are fully labile
J_{kin}	the purely kinetic metal flux
k_a	association rate constant of the reaction M + L ⇌ ML
k_d	dissociation rate constant of ML
${}^jk_{ai}$, ${}^jk_{di}$	the association and dissociation rate constants corresponding to reaction (eq 4)
${}^jK_i$	the equilibrium constants of reaction (eq 4)
L	ligand
ML	metal complex
P	the permeability
α'_j	$(1 + \sum_{i=1}^{j} \sum_{k=1}^{jm} {}^i\varepsilon_k{}^i\beta_k[{}^iL]^k)$, the dynamic degree of complexation of M
${}^j\beta_i$	the cumulative stability constant of the reaction: $M + i^jL \leftrightarrow M^jL_i$
τ	the lifetime of free metal ion in the reaction layer $0 \le x \le \mu$

$^{j}\varepsilon_i$ $D_{M^jL_i}/D_M$, the normalized diffusion coefficient of complex M^jL_i
δ the diffusion layer thickness
$^{j}\xi$ degree of lability of M^jL

Supporting Information Available: Includes the derivation of $\bar{\lambda}_{n_l-1}$ and $^{c}\bar{\lambda}_{n_l-1}$, the dynamic parameter values of Pb(II) species used for simulations in the modified Aquil medium, and the dynamic parameters of Cu(II) species used for flux enhancement studies. This material is available free of charge via the Internet at http://pubs.acs.org.

References and Notes

(1) van Leeuwen, H. P.; Town, R. M.; Buffle, J.; Cleven, R. F. M.; Davison, W.; Puy, J.; van Riemsdijk, W. H.; Sigg, L. *Environ. Sci. Technol.* **2005**, *39*, 8545.

(2) Campbell, P. G. C. In *Metal Speciation and Bioavailability in Aquatic Systems*; Tessier, A., Turner, D. R., Eds.; IUPAC Series on Analytical and Physical Chemistry of Environmental Systems; John Wiley & Sons: Chichester, UK, 1995; Vol. 3, pp 45−102.

(3) van Leeuwen, H. P.; Galceran, J. In *Physicochemical Kinetics and Transport at Biointerfaces*; van Leeuwen, H. P., Köster, W., Eds.; IUPAC Series on Analytical and Physical Chemistry of Environmental Systems; John Wiley & Sons: Chichester, UK, 2004; Vol. 9, pp 113−146.

(4) Wilkinson, K. J.; Buffle, J. In *Physicochemical Kinetics and Transport at Biointerfaces*; van Leeuwen, H. P., Köster, W., Eds.; IUPAC Series on Analytical and Physical Chemistry of Environmental Systems; John Wiley & Sons: Chichester, UK, 2004; Vol. 9, pp 445−533.

(5) Buffle, J.; Tercier-Waeber, M.-L. *Trends Anal. Chem.* **2005**, *24*, 172.

(6) Davison, W.; Zhang, H. *Nature (London)* **1994**, *367*, 546.

(7) Heyrovský, J.; Kuta, J. *Principles of Polarography*; Academic Press: New York, 1966.

(8) Koutecký, J.; Koryta, J. *Electrochim. Acta* **1961**, *3*, 318.

(9) van Leeuwen, H. P. *Environ. Sci. Technol.* **1999**, *33*, 3743.

(10) Galceran, J.; Puy, J.; Salvador, J.; Cecilia, J.; Mas, F.; Garces, J. L. *Phys. Chem. Chem. Phys.* **2003**, *5*, 5091.

(11) Salvador, J.; Garcés, J. L.; Companys, E.; Cecilia, J.; Calceran, J.; Puy, J.; Town, R. M. *J. Phys. Chem. A* **2007**, *111*, 4304.

(12) Alemani, D.; Chopard, B.; Galceran, J.; Buffle, J. *Phys. Chem. Chem. Phys.* **2005**, *7*, 3331.

(13) Alemani, D.; Chopard, B.; Galceran, J.; Buffle, J. *Phys. Chem. Chem. Phys.* **2006**, *8*, 4119.

(14) Brdička, R.; Wiesner, K. *Collect. Czech. Chem. Commun.* **1947**, *12*, 39.

(15) Brdička, R.; Wiesner, K. *Collect. Czech. Chem. Commun.* **1947**, *12*, 138.

(16) Koutecký, J.; Brdička, R *Collect. Czech. Chem. Commun.* **1947**, *12*, 337.

(17) Koutecký, J. *Chem. Listy* **1953**, *47*, 323.

(18) Koutecký, J. *Collect. Czech. Chem. Commun.* **1953**, *18*, 597.

(19) Brdička, R.; Wiesner, K. *Naturwissenshaften* **1943**, *31*, 247.

(20) Brdička, R. *Chem. Listy* **1947**, *41*, 6.

(21) Buffle, J.; Startchev, K.; Galceran, J. *Phys. Chem. Chem. Phys.* **2007**, *9*, 2844.

(22) Zhang, Z.; Buffle, J.; van Leeuwen, H. P. *Langmuir* **2007**, *23*, 5216.

(23) Puy, J.; Cecilia, J.; Galceran, J.; Town, R. M.; van Leeuwen, H. P. *J. Electroanal. Chem.* **2004**, *57*, 121–132.

(24) Zhang, Z.; Buffle, J.; Startchev, K.; Alemani, D. *Environ. Chem.* **2008**, *5*, 204.

(25) Buffle, J.; Zhang, Z.; Startchev, K. *Environ. Sci. Technol.* **2007**, *41*, 7609.

(26) Alemani, D.; Buffle, J.; Zhang, Z.; Galceran, J.; Chopard, B. *Environ. Sci. Technol.* **2008**, *42*, 2021.

(27) Morel, F. M. M.; Ruter, J. G. *J. Phycol.* **1979**, *15*, 135.

(28) Gustafsson, J. P.; *Visual MINTEQ*, ver 2.52; KTH, Dept. of land and water Resources Engineering: Stockholm, Sweden.

(29) Zhang, Z.; Buffle, J.; Town, R. M.; Puy, J.; van Leeuwen, H. P. *J. Phys. Chem. A* **2009**, *113*, 6572.

(30) Martell, A. E.; Smith, R. M. *NIST Critically Selected Stability Constants of Metal Complexes*; NIST: Gaithersburg, MD; Version 7.

JP811429E